International Journal of Energetic Materials and Chemical Propulsion, 20(1):31–43 (2021)

HYDRIDE-DEHYDRIDE FINE ZIRCONIUM POWDERS FOR PYROTECHNICS

Ivan V. Amelichkin,[1,*] Elena M. Knyazeva,[2] Rodion Medvedev,[1] Alexandra V. Muslimova,[3] Roman A. Nefedov,[1] Vladislav V. Orlov,[1] Victor I. Sachkov,[1] Anna S. Sachkova,[2] Oyuna B. Stepanova,[1] & Ilya A. Zhukov[1]

[1]*National Research Tomsk State University, Lenin Ave. 36, 634050 Tomsk, Russia*

[2]*National Research Tomsk Polytechnic University, Lenin Ave. 30, 634050 Tomsk, Russia*

[3]*National Research Nuclear University MEPhI (Moscow Engineering Physics Institute), Russia*

*Address all correspondence to: Ivan V. Amelichkin, National Research Tomsk State University, Lenin Ave. 36, Tomsk 634050, Russia, E-mail: amelichkinivan@gmail.com

Original Manuscript Submitted: 7/8/2020; Final Draft Received: 9/24/2020

In this paper, the possibility of obtaining fine zirconium powders by the hydrogenation-dehydrogenation method is studied. The main parameters of the technological process that allow obtaining fine zirconium powders for pyrotechnics are determined. Hydrogenation and dehydrogenation of the samples are carried out in a rotating quartz tube placed in a furnace at temperatures of 380°C and 850°C, respectively. Zirconium hydride is milled using tungsten carbide balls to eliminate the presence of impurities. Thus it is possible to obtain a fine zirconium powder with a number-average particle size of 4.527 ± 2.650 μm and a specific surface area of 0.231 m^2/g from the initial electrolytic zirconium powder with a number-average particle size of 220 μm and a specific surface area < 0.1 m^2/g. The allowed relative error of measuring the specific surface area is ± 5%. Hence it is possible to reduce the particle size of zirconium powder by 54.6 times without changing the composition.

KEY WORDS: *zirconium, powder, milling, hydrogenation-dehydrogenation, hydride*

1. INTRODUCTION

The properties of pyrotechnic composition (PC) are determined by the nature, ratio, and dispersion of the components. Combustion of PC occurs in a condensed phase, on the surface of metallic fuel; therefore, the physicochemical properties of the metal particle surface have a significant effect on the combustion of PC. The redox reaction in PC leads to the release of energy in the form of heat, light, and sound. The reaction rate depends on the particle morphology (specific surface area, particle size) of the components included in the pyrotechnic mixture, as well as their proportions. Moreover, it is known that with decreasing particle

size, the reaction rate increases, which results in an increase in the rate of energy release (Sarawadekar et al., 2008; Zhang et al., 2011). Thus obtaining finely dispersed metal powders is one of the main tasks of pyrotechnics. Highly active zirconium metal powder is one of the major components in PC, which is widely used in flash compositions, in small-gas and ignition compositions for small-sized products, where combustion stability in small-diameter charges is required (Pourmortazavi et al., 2008; Gromov et al., 2014; Han et al., 2019, 2020).

Finely dispersed zirconium powder (< 40 μm) ignitions occur promptly and at a temperature of 180–200°C. Larger zirconium particles typically require higher temperatures (Lee, 2002; Frost et al., 2008; Badiola et al., 2013).

High purity and finely dispersed zirconium powders are needed to conform to the pyrotechnic requirements. There are various methods for producing finely dispersed zirconium powders, such as thermal reduction of metals, electrolysis of molten salts, oxidation of electrodes, thermal explosion method for production of hydrides (Rosenband et al., 2013), and hydrogenation-dehydrogenation (HDH) (Luo et al., 2017; Choi et al., 2018). Among the above methods, HDH is the most common for producing finely dispersed zirconium powders due to low cost, flexibility, and simplicity of the process (Lustman et al., 1955; Gökelma et al., 2018). A typical HDH process consists of three stages: hydrogenation, milling, and dehydrogenation. The metal-hydride transformation serves only for grinding or imparting special properties and high activity to the powder. The hydrogenation reaction is exothermic and proceeds faster on the surface. The hydride forms directly in the form of a powder, or it is so brittle that it can be easily crushed (Liu et al., 2019). The hydrogenation reaction proceeds with the release of heat and the expansion and deformation of the crystal metallic lattice, and leads to mechanical destruction of the material. During dehydrogenation, zirconium hydride powder is converted to zirconium metal powder. The particle size of the final product depends on the composition and structure of the material, the number of HDH cycles, and the method of grinding zirconium hydride. Zirconium powders are too soft and ductile for mechanical grinding (Lustman et al., 1955). However, zirconium hydride is brittle and easily crushed into powder, which decomposes into metal and hydrogen when it is heated in a vacuum (Kang et al., 2015). Zirconium hydrides are formed at a temperature range from 235°C to 800°C, and the most intensive absorption of hydrogen occurs at 400°C. The hydride formed at 400°C is mainly ZrH_2, while the powder obtained at 800°C is ZrH, but when cooled in hydrogen from 800°C, some of this hydride turns into ZrH_2. The final product is a mixture of these two hydrides (Douglas, 1963). Both hydrides are brittle and can be crushed by traditional methods, for example, in a ball drum. Then zirconium hydride is decomposed in a dynamic vacuum at a temperature from 400°C to 800°C and again milled, sieved through a sieve with the required mesh size, selecting the required fraction of the finished powder (Zhang et al., 2011). However, in the works of Anfilov et al. (2015) and Kuznetsov et al. (2017), in particular, it was shown that during HDH of metal powder, the average mass size of its particles can both decrease or increase depending on the conditions of these processes. Therefore, it is necessary to choose the process conditions that do not lead to sintering between particles with a consequent enlargement of their diameter. This can be achieved by constantly mixing the material in the HDH processes, so a rotating tube furnace was chosen as the main device for conducting experiments. In addition, an important task was to maintain the purity of the product and prevent the formation of impurities in the production process. Thus the aim of our study was to obtain by HDH a zirconium powder with an average particle size of less than 10 μm and the content of impurities as in the source material.

2. EXPERIMENTAL

2.1 Analytical Research Methods

2.1.1 Phase Composition and Structural Characteristics

The determination of phase composition and structural parameters for the samples was carried out at the Center of Materials Science for Collective Use of Tomsk State University, Tomsk (Russian Federation). The study was conducted using an XRD-6000 diffractometer from Shimadzu Corporation (Japan) with CuKα-radiation = 1.54056 Å, and 2O in the range of 10–80°C. The phase composition was analyzed with the use of PDF databases 4+ and the full-profile analysis software PowderCell 2.4.

2.1.2 Elemental Composition

Elemental composition was determined using mass spectroscopy with inductively coupled plasma on an ICP-MS ELAN-9000 DRC-e mass spectrometer (Perkin Elmer, USA). According to the procedure, 10 g of the samples were preliminarily subjected to wet combustion at 450°C with subsequent spraying of the obtained solution into plasma of the inductively coupled discharge. The calibration curve of Au was built within the range of 0.0000001–0.0035% wt.

2.1.3 Particle Size Distribution

The particle size distribution was determined on a sieve vibration analyzer ASV-300 (Russia) by dry sieving. For analysis, we used a set of sieves with holes of diameters of 20, 40, 125, 250, 500 μm, and 1 mm. The mass of the initial sample for sieving was 400–500 g. Shaking was carried out for 30–60 min. Vibration amplitude of the drive plate was from 0.25 to 1.5 mm depending on the weight installed on the plate. Vibration frequency was 1500 Hz. For weighing we used an analytical balance AND HR-250AZ, repeatability (standard deviation) 0.1 mg. The yield of each fraction was calculated and the differential and integral curve of the fractional composition was constructed. The total yield of the product was compared with the mass of the initial sample; the result for processing was taken with a difference between the initial and final masses of less than 3%.

2.1.4 Morphology of Samples

2.1.4.1 Scanning Electron Microscopy Analysis

The zirconium powders obtained by dehydrogenation were analyzed by scanning electron microscopy (SEM). For this purpose, the samples were coated with a gold layer, then SEM micrographs were captured by a VEGA 3 TESCAN scanning electron microscope (Tescan Orsay Holdings, Kohoutovice, Czech Republic) at 10.0 kV. ImageJ was utilized to determine the average particle size as an open-source image analysis program for Macintosh, Windows, and Linux operating systems.

2.1.5 Specific Surface Analysis

The parameters of the porous structure and specific surface area of the samples were analyzed using the TriStar 3020 automatic gas adsorption analyzer. A bulk version of the sorption method

was used. The specific surface was calculated from the isotherm of low temperature sorption of nitrogen vapor. The specific surface of the samples was determined by the Brunauer–Emmett–Teller method by thermal desorption of argon with an internal standard. Before measurements, the samples were degassed in vacuum at a temperature of 240°C for 2 h.

2.2 Sample

Electrolytic zirconium powder was used as raw material for the preparation of finely dispersed zirconium powders. The phase and elemental compositions and particle size distribution of the initial sample were determined by the methods described in Section 2.1.

The chemical composition of the initial powder of zirconium electrolytic (% wt) was: Zr, 99.49; B, 0.05; Na, 0.04; Al, 0.02; P, 0.01; K, 0.02; Sc, 0.03; Ti, 0.20; Fe, 0.03; Cd, 0.05; In, 0.01; Hf, 0.04; and W, 0.00.

The particle size distribution is presented in Table 1 and Fig. 1. The phase composition is presented in Table 2.

TABLE 1: The particle size distribution of the initial powder of zirconium electrolytic

Size of particles, μm	Differential product yield, % wt	Integrated product yield, % wt
< 20	0	0
40–20	0.5	0.5
125–40	19.9	20.4
250–125	32.5	52.9
500–250	38.5	91.4
1000–500	8.6	100
> 1000	0	100

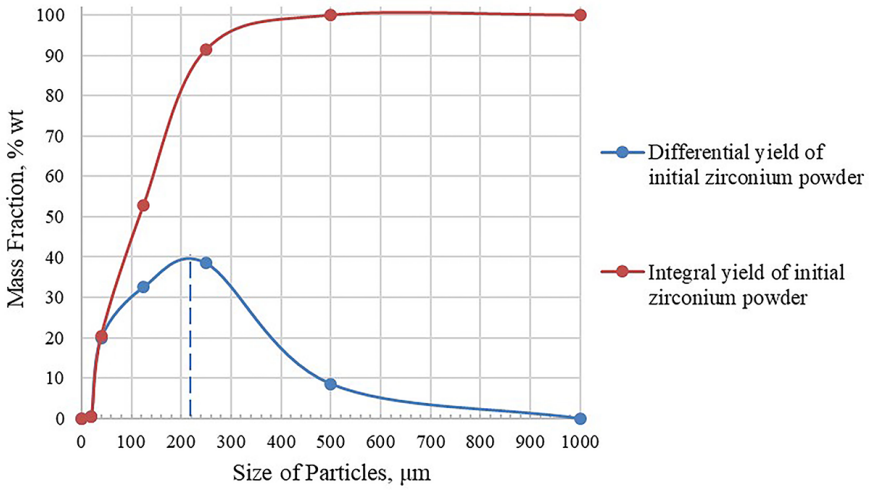

FIG. 1: The particle size distribution of the initial zirconium powder and average particle size

TABLE 2: The phase composition of the initial sample of zirconium powder

Content	Mass fraction, % wt	Lattice parameters, Å	Size of the coherent scattering region, nm
Zr	100	a = 3.2343 c = 5.1498	57

The main fraction of the initial zirconium powder sample was from 500 to 125 μm in size and amounted to 71% wt in total. The yield of the fraction with a particle size of less than 125 μm was 20.4%. The yield of the fraction with a particle size of more than 500 μm was 8.6%. The mean particle size is 220 μm (Fig. 1).

Analysis of the specific surface showed that the initial zirconium powder was quite dense and not porous; its specific surface did not exceed 1 m^2/g. The specific surface was calculated based on the average particle size and was 0.00423 m^2/g.

The phase composition and structural characteristics of the initial sample of zirconium powder are presented in Table 2.

2.3 The HDH Method for Preparation of Fine Zirconium Powder with a Particle Size of Less Than 10 μm

2.3.1 Hydrogenation

Hydrogenation of zirconium powder samples was carried out in a quartz tube placed in a furnace, Nabertherm RSRC 80-750/11, in accordance with the diagram in Fig. 2.

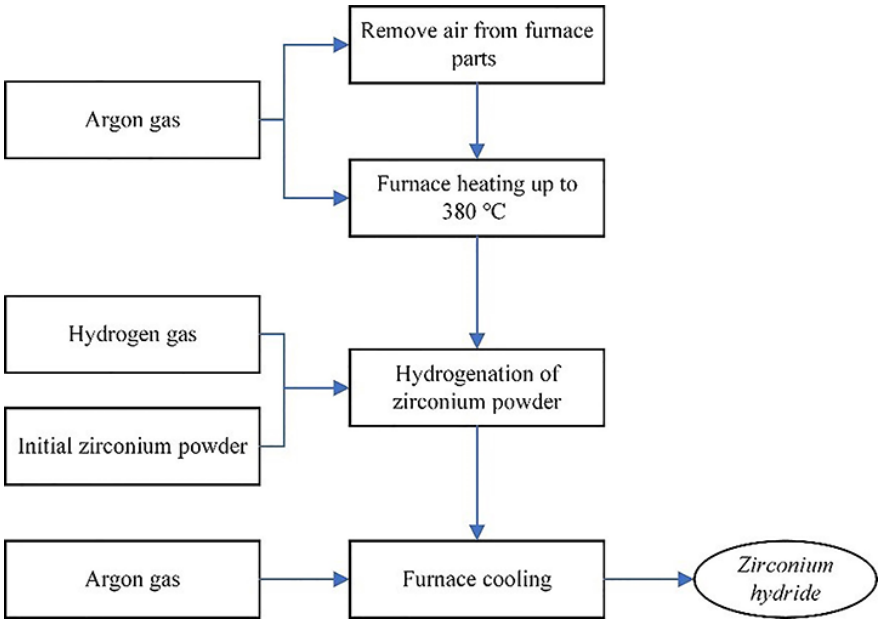

FIG. 2: Scheme of hydrogenation stages

Argon was flown to the furnace to remove air from the quartz tube, receiving tank, feed hopper, and other furnace parts. After that, the initial zirconium powder was fed into the feed hopper. The furnace was heated to 380°C. When the set temperature was reached, the argon flow ceased and hydrogen was flown. The speed of quartz tube rotation and the rotation of the screw conveyor were established, which are necessary for uniform distribution and movement of material through the quartz tube. The material was in the heating zone for 20 minutes. The powder moved through the quartz tube and was accumulated in the receiving tank. At the end of hydrogenation, the heating was turned off, the rotation of the tube and screw feeder was turned off, and the furnace was cooled down to ambient temperature. After that, the receiving tank with the product was removed and transferred to a pressure-tight glove box with an inert atmosphere for further work.

2.3.2 Milling Zirconium Hydride

Zirconium hydride is more crushable than metallic zirconium, so the coefficient of resistance to milling will be much less.

The experiments on milling samples after hydrogenation were carried out in a ball drum mill placed in a pressure-tight glove box with an inert atmosphere (Ar/N_2). The experimental conditions are presented in Table 3.

The type of milling was wet. Heptane was used as a process controlling agent in wet milling because water could lead to hydrolysis of zirconium hydride. The mill drum was made of polypropylene to prevent grinding of the drum material and contamination of the product.

2.3.3 Dehydrogenation

Dehydrogenation of zirconium hydride samples was carried out in a quartz tube placed in a furnace, Nabertherm RSRC 80-750/11, in accordance with the diagram in Fig. 3.

Argon was flown to the furnace to remove air from the quartz tube, receiving tank, feed hopper, and other furnace parts. After that, the initial zirconium powder was fed into the feed

TABLE 3: Zirconium hydride grinding parameters in a drum mill with tungsten carbide balls

Characteristics	**Value**
Drum material	Polypropylene
Grinding drum sizes: Diameter, mm Height, mm	 110 115
Ball material	Tungsten carbide (WC)/Chrome-bearing steel
Ball diameter, mm	2
Total mass of milling balls, g	1300
Mass of mill feed, g	180
Dispersion medium, volume	n-heptane (99.8%), 80 ml
Rotation speed, rpm	120
Time of milling, h	1

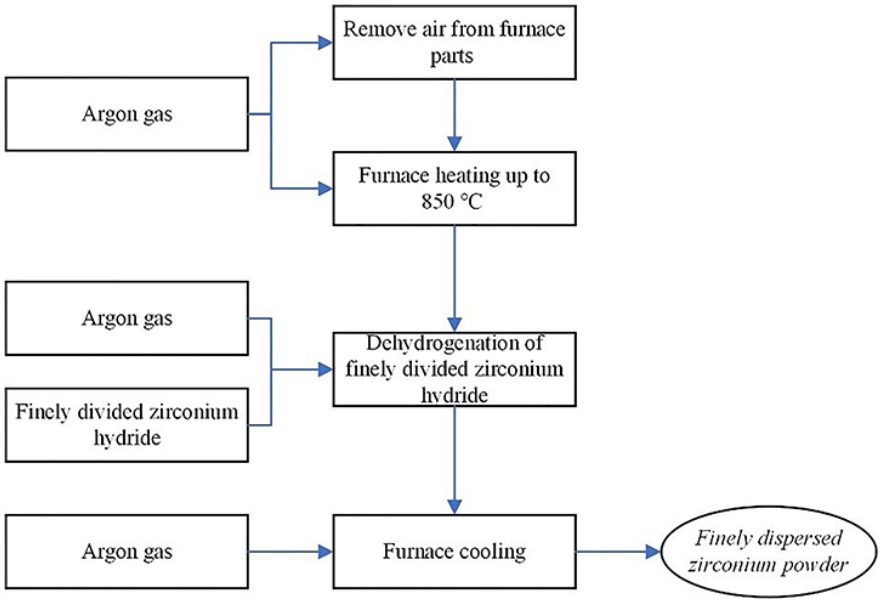

FIG. 3: Scheme of dehydrogenation stages

hopper. The furnace was heated to 850°C. The speed of quartz tube rotation and the rotation of the screw conveyor were established, which are necessary for uniform distribution and movement of material through the quartz tube. The material was in the heating zone for 20 min. The powder moved through the quartz tube and was accumulated in the receiving tank. At the end of dehydrogenation, the heating was turned off, the rotation of the tube and screw feeder was turned off, and the furnace was cooling. After that, the receiving tank with the product was removed and transferred to a pressure-tight glove box with an inert atmosphere for further work.

3. RESULTS

3.1 The Results of the HDH Process

Under these conditions, described in Section 2.3, a series of experiments were conducted that showed repeatability of the results. The particle size distribution of the initial zirconium powder and powder after hydrogenation is presented in Fig. 4.

The change in particle size after the hydrogenation process was not significant. Fractions of hydrogenated powder with particle sizes from 125 to 40 μm, from 250 to 125 μm, and from 500 to 250 μm were 22.6%, 37.8%, and 26.8%, while in the initial powder they were 19.9%, 32.5%, and 38.5%, respectively. However, as can be seen from Fig. 4, there is a positive dynamic of changes in the particle size distribution: a decrease in the content of large fractions with a particle size of 1000 to 250 μm and an increase in the content of small fractions with a particle size of 125 to 20 μm. The metal failure during interaction with hydrogen occurs due to the stretching and breaking of atomic bonds. The work of stretching and breaking bonds leads to the growth of microcracks in the material, accompanied by relaxation of elastic stresses in the volume of their growth and passes into surface energy. It is obvious that the appearance of much lower pressures should lead to the dispersion of metals during the absorption of hydrogen. Each subsequent

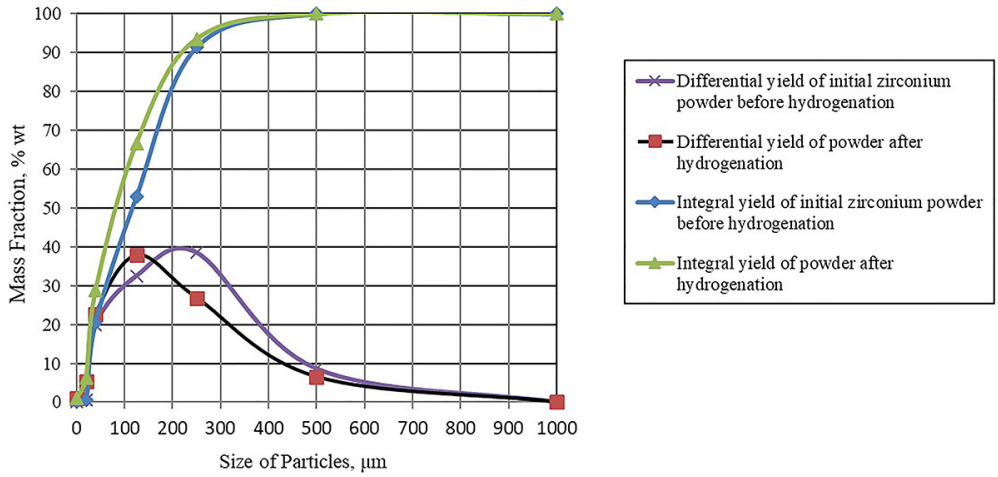

FIG. 4: Particle size distribution of the initial sample of zirconium powder and powder after hydrogenation

hydrogenation cycle is accompanied by the appearance of new stresses, so there is a further development of lattice defects, leading to its destruction and, consequently, to the dispersion of the material.

The phase composition and structural characteristics of the hydrogenated zirconium powder sample are presented in Table 4. According to the results of x-ray phase analysis, the zirconium hydride sample obtained by hydrogenation stage contained 5.4% of the initial zirconium powder. Figure 5 showed the particle size distribution of the hydrogenated powder before and after milling in a ball mill.

During dehydrogenation of zirconium hydride in these conditions, the particle size was decreased by two times. Thus we needed to use zirconium hydride powder with a particle size of less than 20 μm at the dehydrogenation stage to obtain a fine zirconium powder with a particle size of less than 10 μm. For this reason, the milling of the zirconium hydride to a final fineness of less than 20 μm was carried out.

According to the results (Figs. 4 and 5) after milling zirconium hydride with tungsten carbide balls (2 mm), the main fraction belongs to the size class (–20) μm and totals 63% wt, thus this fraction increased by 63.6 times compared with the initial hydride (0.99% wt).

The elemental analysis results of samples are presented in Table 4.

TABLE 4: The phase composition of the milling zirconium powder sample after dehydrogenation

Content	Mass fraction, % wt	Lattice parameters, Å	Size of the coherent scattering region, nm
Zr	5.4	a = 3.2326 c = 5.1489	58
ZrH_2	94.6	a = 3.5183 c = 4.4627	44

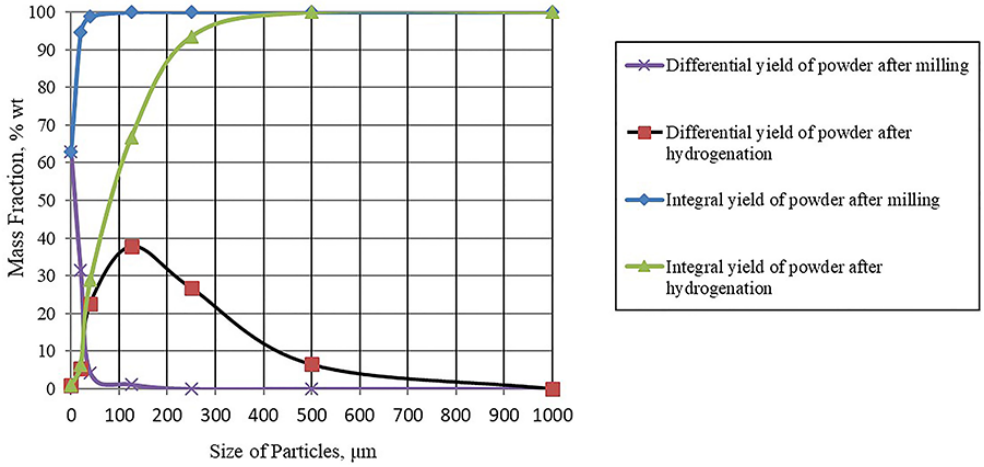

FIG. 5: Particle size distribution of the hydrogenated powder before and after milling in a ball mill

According to elemental analysis (Table 5), the zirconium hydride sample, which was milled in a ball mill with steel balls, contained 0.24% wt iron impurities, and the iron content in the initial powder was 0.03% wt. There were no impurities in the process of milling zirconium hydride with balls of tungsten carbide since the material of the balls did not grind. Thus, for finer milling and maintaining the purity of the product, it is necessary to use milling balls of tungsten carbide.

TABLE 5: The elemental composition of the initial sample and samples after milling

Content	Initial zirconium powder	Zirconium hydride powder after milling with tungsten carbide balls	Zirconium hydride powder after milling with steel balls
	Mass fraction, % wt		
B	0.05	0.05	0.05
Na	0.04	0.04	0.04
Al	0.02	0.02	0.02
P	0.01	0.01	0.01
K	0.02	0.02	0.02
Sc	0.03	0.03	0.03
Ti	0.20	0.20	0.20
Fe	0.03	0.03	0.24
Zr	99.49	99.49	99.28
Cd	0.05	0.05	0.05
In	0.01	0.01	0.01
Hf	0.04	0.04	0.04
W	0.00	0.00	0.00

After the milling stage in a ball mill, dehydrogenation of the zirconium hydride samples was carried out according to the procedure described in Section 2.3.3.

According to SEM (Fig. 6), the sample of zirconium powder obtained by the HDH process was a loose powder with a developed surface, which consisted of clusters of fragmented particles. The particle shape was fragmentation due to the milling of zirconium hydride in a ball mill.

The particle size was measured as the average from minimum and maximum Feret diameters using ImageJ software. The number of the sampled particles analyzed by ImageJ are 176 for image A (732× magnification), 146 for image B (1930× magnification), 49 for image C (5590× magnification), and 43 for image D (8080× magnification). The particle size was approximately from 20 to 0.5 μm. For image A the mean particle size was 5.062 μm, standard deviation ± 2.805; for image B, 4.751 μm, standard deviation ± 2.594; for C, 3.260 μm, standard deviation ± 1.913; and for D, 3.031 μm, standard deviation ± 1.830. Taking into account all the images, the mean particle size was 4.527 μm, standard deviation ± 2.650. Thus, after milling by the method, the mean particle size decreased from 220 μm to 4.527 μm; that is, in the product this value became 54.6 times less than in the initial powder. When calculating the specific surface area values, the density of the zirconium powder was assumed to be 6.506 g/cm^3. The specific

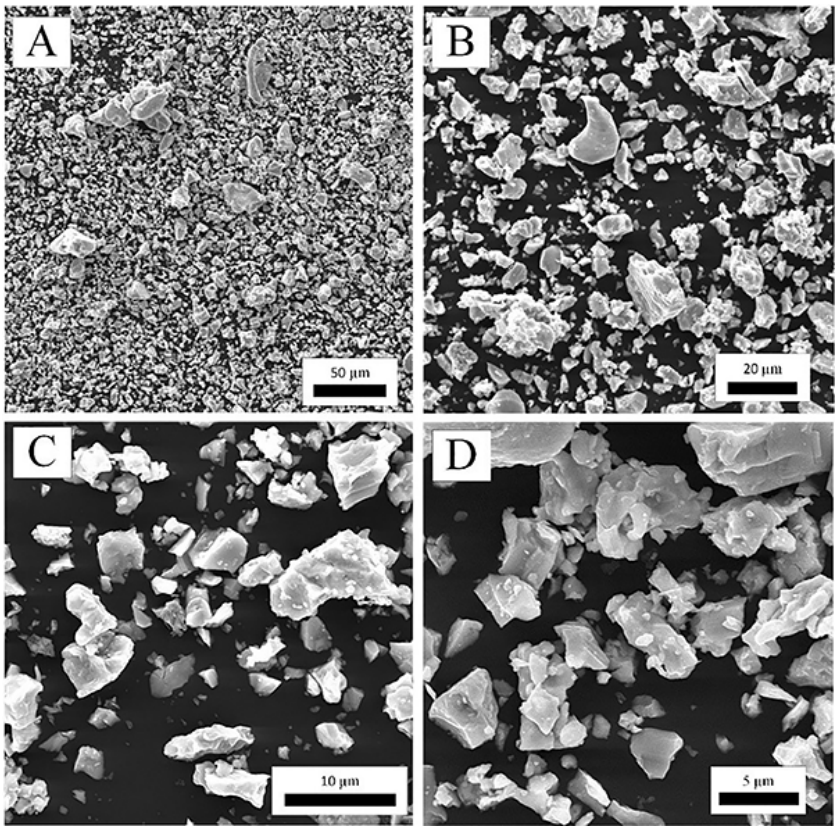

FIG. 6: SEM images of the HDH fine zirconium powder. A: 732× magnification, scale length 50 μm; B: 1930× magnification, scale length 20 μm; C: 5590× magnification, scale length 10 μm; D: 8080× magnification, scale length 5 μm.

surface was calculated based on the average particle size and was 0.231 m^2/g. Comparison of the initial powder and the final product is presented in Table 6. The phase composition and structural characteristics of the HDH fine zirconium powder are presented in Table 7.

According to the results of X-ray phase analysis, the zirconium sample obtained by the HDH method contained zirconium hydride impurities (4%).

4. CONCLUSIONS

Hydride-dehydride fine zirconium powder was obtained with a mean particle size of 4.527 ± 2.650 μm and a specific surface area value of 0.231 m^2/g from the initial electrolytic zirconium powder with a mean particle size of 220 μm and a specific surface area value of 0.00423 m^2/g. Thus it was possible to reduce the particle size of zirconium powder by 54.6 times. The particle shape was fragmentation due to the milling of zirconium hydride in a ball mill.

The impurity content in the product (HDH fine zirconium powder) was the same as in the initial electrolytic zirconium powder. The HDH fine zirconium powder was of high quality, and new impurities did not form due to the purity of the HDH process and moreover, due to the use of tungsten carbide balls and a polypropylene drum at the milling stage of zirconium hydride.

Based on the analysis of the experimental data, fine zirconium powders obtained by the HDH method can be used in the manufacture of pyrotechnic materials due to the fine particle size and purity of the powder.

ACKNOWLEDGMENT

This research was supported by Ministry of Science and Higher Education of the Russian Federation, project No. 0721-2020-0028.

TABLE 6: Comparison of the characteristics of the initial zirconium powder and product (HDH fine zirconium powder)

Characteristics	Initial zirconium powder	HDH fine zirconium powder
Mean particle size, μm	220	4.026
Specific surface, m^2/g	0.00423	0.231

TABLE 7: The phase composition of the milling zirconium powder sample after dehydrogenation

Content	Mass fraction, % wt	Lattice parameters, Å	Size of the coherent scattering region, nm
Zr	96	a = 3.2397 c = 5.1633	48
ZrH	4	a = 4.5915 c = 4.9575	59

REFERENCES

Anfilov, N.V., Kuznetsov, A.A., Berezhko, P.G., Tarasova, A.I., Tsareva, I.A., Mokrushin, V.V., and Malkov, I.L., Application of Metal Hydrides as Pore-Forming Agents for Obtaining Metal Foams, *J. Alloys Compounds*, vol. **645**, pp. S132–S135, 2015.

Badiola, C. and Dreizin, E.L., Combustion of Micron-Sized Particles of Titanium and Zirconium, *Proc. Combust. Inst.*, vol. **34**, no. 2, pp. 2237–2243, 2013.

Douglas, T.B., High-Temperature Thermodynamic Functions for Zirconium and Unsaturated Zirconium Hydrides, *J. Res. Natl. Bureau Standards*, vol. **67**(A), pp. 403–426, 1963.

Frost, D.L., Cairns, M., Goroshin, S., and Zhang, F., Reaction of Titanium and Zirconium Particles in Cylindrical Explosive Charges, *AIP Conf. Proc., Am. Inst. Phys.*, vol. **955**, no. 1, pp. 781–784, 2007.

Gökelma, M., Celik, D., Tazegul, O., Cimenoglu, H., and Friedrich, B., Characteristics of Ti_6Al_4V Powders Recycled from Turnings via the HDH Technique, *Metals*, vol. **8**, no. 5, p. 336, 2018.

Gromov, A., DeLuca, L.T., Il'in, A.P., Teipel, U., Petrova, A., and Prokopiev, D., Nanometals in Energetic Systems: Achievements and Future, *Int. J. Energetic Mater. Chem. Propuls.*, vol. **13**, no. 5, pp. 399–419, 2014.

Han, B., Gnanaprakash, K., Park, Y., and Yoh, J.J., Understanding the Effects of Hygrothermal Aging on Thermo-Chemical Behaviour of Zr-Ni based Pyrotechnic Delay Composition, *Fuel*, vol. **281**, p. 118776, 2020.

Han, B.H., Kim, Y., Jang, S., Yoo, J., and Yoh, J.J., Thermochemical Characterization of Zr/Fe_2O_3 Pyrotechnic Mixture under Natural Aging Conditions, *J. Appl. Phys.*, vol. **126**, no. 10, p. 105113, 2019.

He, Z., Hayat, M.D., Huang, S., Wang, X., and Cao, P., Physicochemical Characterization of PbO_2 Coatings Electrosynthesised from a Methanesulfonate Electrolytic Solution, *J. Electrochem. Soc.*, vol. **165**, no. 14, pp. D1–D6, 2018.

Kang, J.-G., Jiang, Y., He, Y.-H., and Gao, H., Fabrication and Properties Characterization of Zr Powder by Hydrogenation-Dehydrogenation Combined Method, vol. **20**, pp. 655–660, 2015.

Kuznetsov, A.A., Berezhko, P.G., Kunavin, S.M., Zhilkin, E.V., Tsarev, M.V., Yaroshenko, V.V., and Mityashin, S.A., Application of Acoustic Emission Method to Study Metallic Titanium Hydrogenation Process, *Int. J. Hydrogen Energy*, vol. **42**, no. 35, pp. 22628–22632, 2017.

Lee, J.-S., Thermal Properties and Firing Characteristics of the $Zr/KClO_4$/Viton A Priming Compositions, *Thermochimica Acta*, vols. **392–393**, pp. 147–152, 2002.

Liu, H., Lian, L., and Liu, Y., Vacuum Activation Assisted Hydrogenation-Dehydrogenation for Preparing High-Quality Zirconium Powder, *Mater. Manufacturing Processes*, pp. 1–7, 2019.

Luo, S.D. and Qian, M., Microwave Processing of Titanium and Titanium Alloys for Structural, Biomedical and Shape Memory Applications: Current Status and Challenges, *Mater. Manufacturing Processes*, vol. **33**, no. 1, pp. 35–49, 2017.

Lustman, B. and Kerze, F., Eds., *The Metallurgy of Zirconium*, vol. **4**, New York: McGraw-Hill, 1955.

Pourmortazavi, S.M., Hosseini, S.G., Hajimirsadeghi, S.S., and Alamdari, R.F., Investigation on Thermal Analysis of Binary Zirconium/Oxidant Pyrotechnic Systems, *Combust. Sci. Technol.*, vol. **180**, no. 12, pp. 2093–2102, 2008.

Rosenband, V. and Gany, A., Thermal Explosion Synthesis of Titanium Hydride Powders, *Int. J. Energetic Mater. Chem. Propuls.*, vol. **12**, no. 4, pp. 347–359, 2013.

Sarawadekar, R. and Agrawal, J., Nanomaterials in Pyrotechnics, *Defence Sci. J.*, vol. **58**, no. 4, pp. 486–495, 2008.

Zhang, H., Shen, H., Che, X., and Wang, L., Zirconium Powder Production through Hydrogenation and Dehydrogenation Process, *Xiyou Jinshu/Chinese J. Rare Metals*, vol. **35**, pp. 417–421, 2011.

Zhang, Q., Yi, Y., Kang, X., Luo, J., Tang, Y., Li, K., Effects of Zirconium Size on Combustion Characteristics of Zr/KP Pyrotechnics, *High Power Laser Particle Beams*, vol. **23**, no. 7, pp. 1867–1872, 2011.